

Journal Pre-proofs

Novel quinolin-4(1*H*)-one derivatives as multi-effective aldose reductase inhibitors for treatment of diabetic complications: synthesis, biological evaluation, and molecular modeling studies

Zhongfei Han, Junkai Zhu, Yunnan Zhang, Ying Zhang, Huiyun Zhang, Gang Qi, Changjin Zhu, Xin Hao

PII: S0960-894X(20)30190-6
DOI: <https://doi.org/10.1016/j.bmcl.2020.127101>
Reference: BMCL 127101

To appear in: *Bioorganic & Medicinal Chemistry Letters*

Received Date: 3 January 2020
Revised Date: 4 March 2020
Accepted Date: 7 March 2020

Please cite this article as: Han, Z., Zhu, J., Zhang, Y., Zhang, Y., Zhang, H., Qi, G., Zhu, C., Hao, X., Novel quinolin-4(1*H*)-one derivatives as multi-effective aldose reductase inhibitors for treatment of diabetic complications: synthesis, biological evaluation, and molecular modeling studies, *Bioorganic & Medicinal Chemistry Letters* (2020), doi: <https://doi.org/10.1016/j.bmcl.2020.127101>

This is a PDF file of an article that has undergone enhancements after acceptance, such as the addition of a cover page and metadata, and formatting for readability, but it is not yet the definitive version of record. This version will undergo additional copyediting, typesetting and review before it is published in its final form, but we are providing this version to give early visibility of the article. Please note that, during the production process, errors may be discovered which could affect the content, and all legal disclaimers that apply to the journal pertain.

© 2020 Published by Elsevier Ltd.



Novel quinolin-4(1H)-one derivatives as multi-effective aldose reductase inhibitors for treatment of diabetic complications: synthesis, biological evaluation, and molecular modeling studies

Zhongfei Han^{a, b}, Junkai Zhu^a, Yunnan Zhang^a, Ying Zhang^a, Huiyun Zhang^a, Gang Qi^a, Changjin Zhu^b and Xin Hao^{a*}

^aFaculty of Chemistry and Chemical Engineering, Yancheng Institute of Technology, Yancheng, China; ^bDepartment of Applied Chemistry, Beijing Institute of Technology, Beijing, China.

*Corresponding author. E-mail: haoxin@ycit.edu.cn.

Novel quinolin-4(1H)-one derivatives with hydroxamic acid or acyl-sulfonamide used as the bioisostere of acetic acid were developed as multi-effective aldose reductase inhibitors. Most of these 24 derivatives, having a N1 benzyl side chain and substituted C3 acetic acid or its bioisostere on the core structure, were found to be potent and selective aldose reductase inhibitors with submicromolar IC₅₀ values against AKR1B1 and no more than 38.6% inhibition percentage to AKR1A1 at the concentration of 10 μM. Particularly, **6j** was the most active compound with IC₅₀ value of 0.057 μM. Some of the derivatives showed not only good activity in the AKR1B1 inhibition but also potent antioxidant activity. Compounds **6j** and **7j** with excellent inhibitory activity of AKR1B1, were also confirmed to be an equivalent antioxidant comparable with Trolox. Moreover, compound **7j** with the acetic acid bioisostere moiety was proved to be potent inhibitors of AKR1B1 whilst retaining a favorable physicochemical profile, which suggested hydroxamic acid was a good bioisosteric replacement of acetic acid in the ARIs design. Structure activity relationship and molecular docking study highlighted the importance of hydroxamic acid head group along with phenolic hydroxyl substituents in N1 side chain of the scaffold for the construction of potent and multifunctional ARIs with good physicochemical profile.

Aldose reductase inhibitors; quinolin-4(1H)-one; antioxidant activity; bioisostere.

Diabetes mellitus (DM), companied with cardiovascular and cancer, are recognized as the three most mainly reasons of human death. All form of DM, including type I and type II, are characterized by hyperglycaemia and the development of chronic diabetic complications, such as nephropathy, cataracts and retinopathy.^{1,2} Based on IDF statistical data, over 256 million people worldwide were suffering diabetes mellitus and this figure would increase steadily to 366 million by 2030.³ Accordingly, both two kinds of diabetes are vulnerable to chronic diabetic complications, and

which are the major threaten faced by diabetic patients. More and more evidences have demonstrated that aldose reductase (AKR1B1, EC1.1.1.21) served as a prominent factor for the onset and progression of chronic diabetic complications. AKR1B1 accompanied with NADPH as coenzyme catalyzes the reduction of glucose to sorbitol in the first and rate-limiting step of the polyol pathway (**Fig. 1**), following with sorbitol dehydrogenase dehydrogenase (SDH) oxidizes sorbitol to fructose.⁴⁻⁶ This glucose metabolism pathway is considered as the leading pathogenesis of the diabetic complications. Normally, the AKR1B1 has little activity and only 3% of glucose metabolize through this pathway. However, under hyperglycemia, the activity of AKR1B1 is stimulated and this figure could rise up to 33% in tissues demonstrating insulin-independent uptake of glucose, such as lens, kidney, retina, and peripheral nerves.^{6,7} The increased glucose metabolism through polyol pathway directly results in various cellular stress conditions, which provide the underlying mechanism of chronic diabetic complications. Furthermore, the physiological role of aldose reductase in the reduction of toxic aldehydes is the key step in the propagation of oxidative-stress induced inflammation, which was identified as an important factor to promote the development of diabetic complications.^{5,8,9} Concurrently, research evidences identified that AKR1B1 was also served as a key mediator in a number of inflammation induced pathologies, such as sepsis, asthma and various type of cancer.

10-12

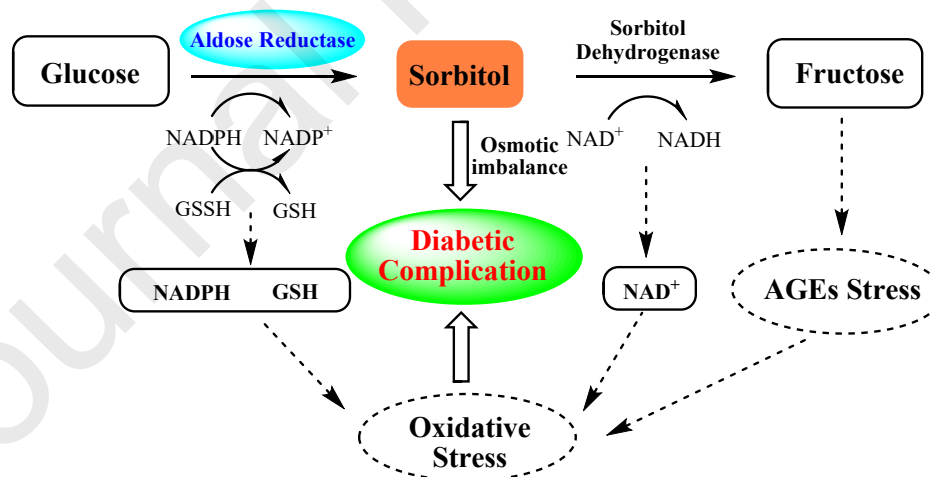


Figure 1. Polyol pathway of glucose metabolism.

Considering the large spectrum of AKR1B1-related pathologies, aldose reductase inhibitors (ARIs) hold great promise for therapeutic intervention.¹³ Numerous structurally different ARIs have been developed and some of them are present in **Fig. 2**.^{14,15} Although a number of ARIs was developed and some of them endowed with excellent inhibitory activity, epalrestat is the only ARI which has passed through clinical trials. Due to the poor clinical efficacy, epalrestat has not pass the FDA and

EMA approval, and it is only available for the therapy in Japan and more recently in China and India.¹² Most of those ARIs that appeared to be promising have not yet succeeded in the clinical trials mainly due to low in vivo efficacies, adverse side effects or pharmacokinetic drawbacks.¹⁶ Carboxylic inhibitors are potent ARIs owing to the high affinity to the positively charged region of the AKR1B1 active site, however, lower pKa values hinder membrane permeability under physiological pH conditions and lead to a poor pharmacokinetic profile.^{12,17} The side effects, typically found in hydantoin inhibitors, are the major obstacles faced by spiroimides during clinical trials. The main reason of the side effects is the off-target inhibition of the closely related aldehyde reductase enzyme (AKR1A1; EC1.1.1.2), which serves as a key role in particularly catalytic metabolizing toxic aldehydes.¹⁸ Therefore, reducing the inhibitory activity of ARIs against AKR1A1 could avoid some undesirable side effects.

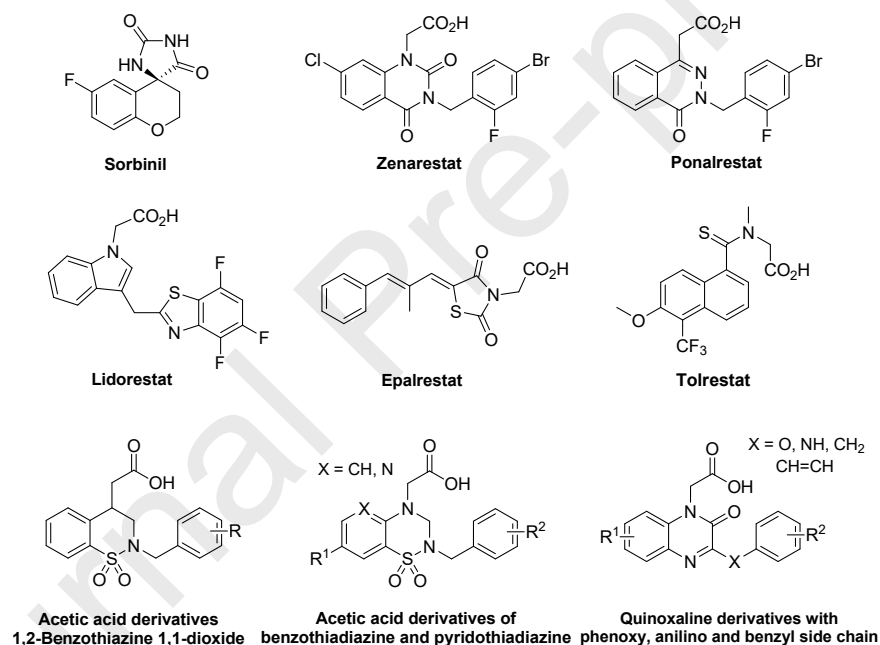
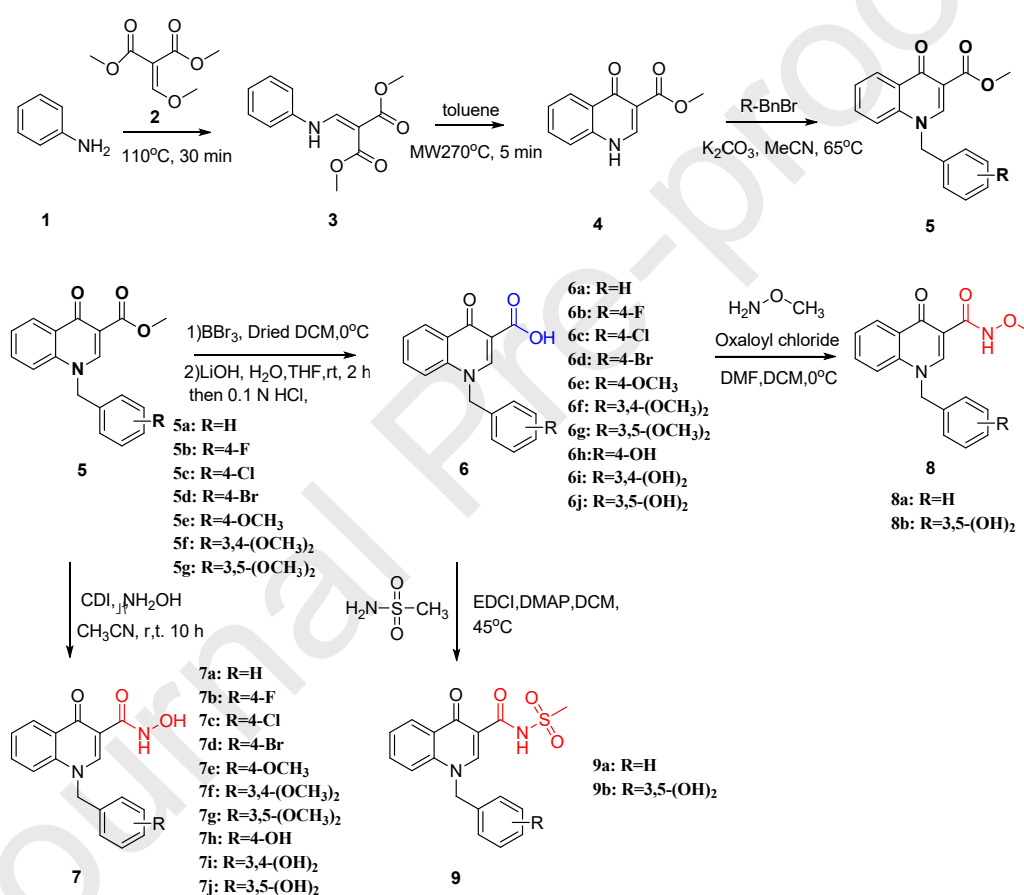


Figure 2. Structures of some ARIs.

We have developed several groups of carboxylic acid ARIs previously and most of them were endowed with significant inhibitory activity and antioxidant activity.^{8,19-23} In the present study, novel quinolin-4(1*H*)-one derivatives with hydroxamic acid or acyl-sulfonamides moiety used as bioisostere of acetic acid were designed and synthesized to optimize the pharmacokinetics of carboxylic inhibitors.

The synthetic compounds with a carboxylate substituent or its bioisostere moiety at C3 position and a variety of aromatic substituents at N1 side chain of the quinolin-4(1*H*)-one scaffold were prepared as **Scheme 1** described. The dimethyl 2-((phenylamino)methylene) malonate **3** was synthesized by aniline **1** and dimethyl 2-(methoxymethylene)malonate **2**, and then the acylation product **3** formed methyl

4-oxo-1,4-dihydroquinoline-3-carboxylate **4** through ring-closure reaction. The N1 position of compound **4** was substituted with different benzyl bromide to form 1-benzyl-4-oxo-1,4-dihydro-quinoline-3-carboxylate **5** as key intermediate for obtaining various target compounds (**6**, **7**, **8** and **9**). Acylation of compound **5** with hydroxylamine yielded target compounds **7a-j**. Hydrolysis of substituted compound **5** with lithium hydroxide obtained the target carboxylic acid compounds **6a-j**. Moreover, Acylation of compounds **6a** and **6j** with *O*-methylhydroxylamine obtained **8a** and **8b** respectively. Similarly, acylation of compounds **6a** and **6j** with methanesulfonamide obtained **9a** and **9b**. The detail of the synthetic procedure was showed in supplementary materials.

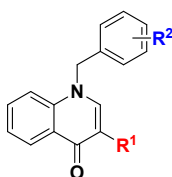


Scheme 1. The synthetic route of target compounds.

Our previous study suggested that the N1-benzyl side chain and C3-acetic acid group on the core structure are essential to obtain an excellent ARI, therefore, those structure features are maintained in the present work. Meanwhile, the phenolic hydroxyl which always endowed with antioxidant activity was introduced to the core structure of ARIs to attach anti-oxidative properties of the ARIs. Furthermore, novel derivatives with hydroxamic acid or acyl-sulfonamides moiety used as bioisostere of acetic acid were also designed to optimize pharmacokinetics of the carboxylic acid

inhibitor.

Table 1. Biological activity of target compounds.



Cpd.	substituent		IC ₅₀ (μM) ^a	Inhib(%) ^b		DPPH sca. %		
	R ¹	R ²		AKR1B1	AKR1A1	100 μM	50 μM	10 μM
6a	-COOH	H	11.017 ± 1.077	5.8	20.3 ± 0.7	*	*	
6b	-COOH	4-F	0.154 ± 0.012	30.2	21.4 ± 0.9	*	*	
6c	-COOH	4-Cl	0.321 ± 0.028	18.3	28.7 ± 1.1	*	*	
6d	-COOH	4-Br	1.528 ± 0.107	20.1	25.4 ± 0.9	*	*	
6e	-COOH	4-OCH ₃	12.031 ± 1.023	21.4	30.5 ± 1.2	*	*	
6f	-COOH	3,4-(OCH ₃) ₂	10.587 ± 1.005	24.8	32.2 ± 1.3	*	*	
6g	-COOH	3,5-(OCH ₃) ₂	9.875 ± 0.928	30.1	47.6 ± 2.0	*	*	
6h	-COOH	4-OH	0.098 ± 0.012	37.5	62.7 ± 2.7	30.4 ± 0.7	14.6 ± 0.2	
6i	-COOH	3,4-(OH) ₂	0.251 ± 0.022	38.6	87.1 ± 3.4	61.9 ± 1.2	44.9 ± 2.1	
6j	-COOH	3,5-(OH) ₂	0.057 ± 0.005	36.6	92.4 ± 3.3	71.1 ± 1.5	51.7 ± 2.5	
7a	-CONHOH	H	12.578 ± 1.069	7.1	27.1 ± 0.9	*	*	
7b	-CONHOH	4-F	0.237 ± 0.023	24.1	32.1 ± 1.1	*	*	
7c	-CONHOH	4-Cl	0.626 ± 0.059	26.5	31.7 ± 1.0	*	*	
7d	-CONHOH	4-Br	2.487 ± 0.186	17.6	27.6 ± 0.8	*	*	
7e	-CONHOH	4-OCH ₃	12.515 ± 1.089	7.6	34.1 ± 1.3	*	*	
7f	-CONHOH	3,4-(OCH ₃) ₂	13.578 ± 1.039	10.5	39.1 ± 1.4	*	*	
7g	-CONHOH	3,5-(OCH ₃) ₂	15.614 ± 1.202	17.2	41.3 ± 1.5	*	*	
7h	-CONHOH	4-OH	0.107 ± 0.008	34.6	74.9 ± 2.4	51.1 ± 1.9	32.3 ± 1.5	
7i	-CONHOH	3,4-(OH) ₂	0.287 ± 0.215	25.4	88.1 ± 3.1	65.1 ± 2.4	51.1 ± 2.0	
7j	-CONHOH	3,5-(OH) ₂	0.065 ± 0.005	27.4	91.0 ± 3.1	72.4 ± 2.6	57.8 ± 2.1	
8a	-CONHOCH ₃	H	12.781 ± 1.163	5.1	25.2 ± 0.8	*	*	
8b	-CONHOCH ₃	3,5-(OH) ₂	0.689 ± 0.057	21.7	88.7 ± 3.0	55.8 ± 2.4	42.7 ± 1.8	
9a	-CONHSO ₂ CH ₃	H	15.034 ± 1.353	7.9	28.7 ± 1.1	*	*	
9b	-CONHSO ₂ CH ₃	3,5-(OH) ₂	0.112 ± 0.010	24.7	79.4 ± 3.1	64.7 ± 3.1	33.6 ± 1.1	
epalrestat			0.081 ± 0.007	43.1	*	*	*	
Trolox					94.2 ± 1.9	84.1 ± 1.2	77.2 ± 0.2	

^a IC₅₀ values represent the concentration required to produce 50% enzyme inhibition.

^b The inhibitory effect was estimated at a concentration of 10 μM.

* Not tested.

All target compounds presented in **Table 1** were evaluated for their inhibitory activity of AKR1B1 extracted from rat lenses, and the selectivity for the AKR1B1 inhibition of the targets compounds were tested through the identification of

inhibitory activity against AKR1A1 which isolated from rat kidneys. IC_{50} and the percentage of enzyme inhibition (%) were applied to express the test results of AKR1B1 and AKR1A1 inhibition respectively, which were summarized in **Table 1**.

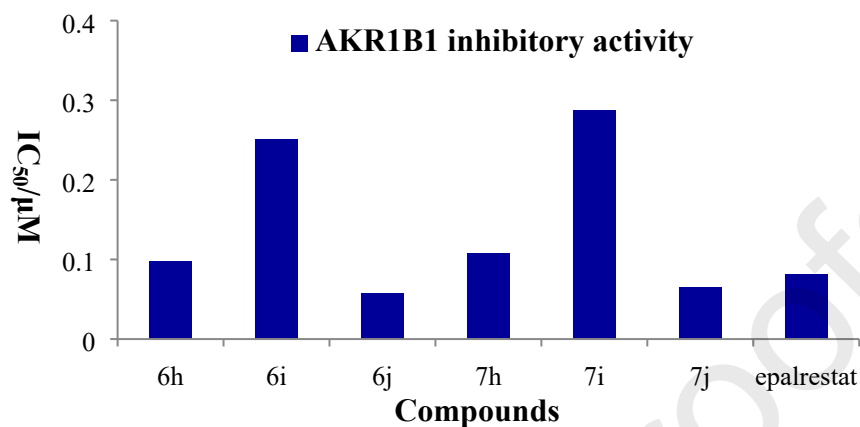


Figure 3. AKR1B1 inhibitory activity of some ARIs.

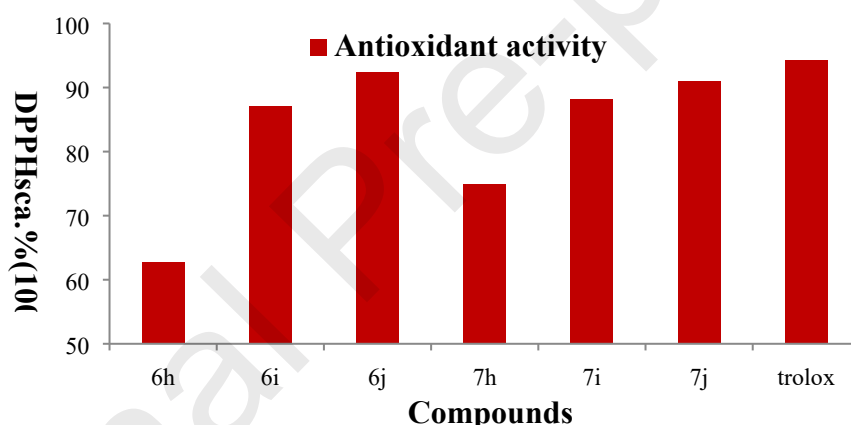


Figure 4. Antioxidant activity of some ARIs.

Most of the quinolin-4(1*H*)-one derivatives showed significant AKR1B1 inhibition and selectivity. Of all the compounds, 1-(3,5-dihydroxybenzyl)-4-oxo-1,4-dihydroquinoline-3-carboxylic acid **6j** was the most active with an IC_{50} value of 0.057 μM , and it was more potent than epalrestat. In the carboxyl series compounds **6a-j**, it was found that the introduction of phenolic hydroxyl or methoxyl to the N1 aryl side chain of **6a** could enhance the inhibitory activity, and phenolic hydroxyl showed better enhancement. Compounds **6e**, **6f** and **6g** having one or two methoxyl on the N1-aryl side chain displayed relatively low AKR1B1 inhibition with IC_{50} values ranging from 9.875 to 12.031 μM . Compounds **6h**, **6i** and **6j** obtained after demethylation showed an obvious enhancement on AKR1B1 inhibition with IC_{50} values in the range from 0.057 to 0.251 μM . Moreover, the introduction of the

halogen substituent F, Cl or Br to N1-aryl group could also largely increase the inhibitory activity. The effect of halogen substituent on AKR1B1 inhibition was in the rank order of 4-F > 4-Cl > 4-Br and the corresponding IC₅₀ value was 0.154 μM, 0.321 μM and 1.528 μM, respectively. Besides, as shown in **Fig. 3**, it was encouraging to find that the inhibitory activity of AKR1B1 was remained when the carboxyl moiety of the quinolin-4(1*H*)-one derivative was replaced to hydroxamic acid group—by comparing the inhibitory activity of compounds **6h-j** and **7h-j**. Particularly, hydroxamic acid compound **7j** having two phenolic hydroxyl groups in N1-aryl side chain was endowed with significant AKR1B1 inhibitory activity with an IC₅₀ value of 0.065 μM. The inhibitory activity was almost equivalent to that of the corresponding carboxylic acid **6j**, which suggested that the strategy of bioisostere in the present study was feasible. Analysis of the structure–activity relationship (SAR) indicated that the introduction of phenolic hydroxyl and or halogen substituent to N1 aryl side chain was also effective in hydroxamic acid series compounds derivatives **7a-j**.

Meanwhile, other two bioisostere strategies were also designed. The results indicated that the substitution *N*-methoxyacetamide or *N*-methylsulfonyl acetamide at the C3 position would result in an obviously loss of AKR1B1 inhibition. The *N*-methoxyacetamide derivative **8a** without structural modification had weak inhibitory activity with an IC₅₀ value of 12.781 μM and **8b** having two phenolic hydroxyl groups in N1-aryl side chain showed moderate AKR1B1 inhibition with an IC₅₀ value of 0.689 μM. Similarly, the *N*-(methylsulfonyl) acetamide derivative **9a** had a weak inhibition activity with an IC₅₀ value of 15.034 μM and **9b** with two phenolic hydroxyl groups at N1 position showed an IC₅₀ value of 0.112 μM. Finally, the selectivity for the AKR1B1 inhibition of all the target compounds was determined, and the results indicated that the compounds had an excellent selectivity with no more than 38.6% inhibition percentage against ~~AKR1B1~~ AKR1A1 under 10 μM concentration.

The antioxidant properties of the synthesized compounds containing the phenolic hydroxyl group were also investigated in the present work and 6-hydroxy-2,5,7,8-chroman-2-carboxylic acid (Trolox) was employed as a positive control. As shown in **Table 1**, all derivatives showed good DPPH radical scavenging activity ranging from 20.3 to 92.4% at the concentration of 100 μM. Of all tested compounds, **6j** with phenolic 3,5-dihydroxyl on the N1-aryl ring showed the best scavenging activity, that is, 92.4%, 71.1%, and 51.7% at concentrations of 100 μM, 50 μM and 10 μM respectively, which had an commensurate activity compared with Trolox at high concentrations. SAR study of compounds (**6e** vs **6h**, **6f** vs **6i**, **6g** vs **6j**,

and **7g** vs **7j**) indicated that the demethylation of methoxyl on N1-aryl side chain could improve the radical scavenging activity significantly. The position of phenolic hydroxyl also had an effect on inhibitory activity, and the phenolic 3,5-dihydroxyl substituent was the most effective on activity enhancement when comparing all the phenolic hydroxyl derivatives. Moreover, comparison of compounds **6b-d** revealed that the halogen substituent had little impact on the radical scavenging activity. As shown in **Fig. 4**, the replacement of carboxyl moiety by its bioisostere had little impact on the antioxidant activity, which could be concluded by comparing the radical scavenging activity of compounds **6h-j** and **7h-j**.

The lipophilicity of compound plays a crucial role during the structural optimization step in the discovery of lead compound. Besides the biological activity, good lipophilicity could also improve the potency of compounds. In this study, lipid-water partition coefficient ($\text{LogD}_{7.4}$) and pKa value at physiological pH were employed to evaluate the lipophilicity of compounds. As shown in **Table 2**, the $\text{logD}_{7.4}$ values were tested through a miniaturized 1-octanol/buffer shake flask assay followed by HPLC analysis. Meanwhile, computer simulation was also used to predict $\text{logD}_{7.4}$ and the pKa value at physiological pH. The results showed that better lipophilicity was detected when the carboxylic acid moiety of quinilin-4(1*H*)-one derivative was replaced by hydroxamic acid group. Particularly, the partition ratio of **7j** in 1-octanol: buffer is 0.57, 2.32 times that of **6j**, and the partition ratio of **7a** is 1.87 times that of **6a**. Moreover, the hydroxamic acid compounds **7a** and **7j** were endowed with a higher pKa value than that of the corresponding carboxylic acid compounds **6a** and **6j**. The calculative pKa values of **7a** and **7j** were 8.93 and 8.73 respectively, which suggested that the hydroxamic acid derivatives would exist in molecular form at physiological pH and would be endowed with better cell membrane permeability. In addition, the lipophilicity would decrease when carboxyl group changed to N-methoxyacetamide or N-methylsulfonyl acetamide. In a word, bioisosteric replacement is an effective strategy to optimize the physicochemical profile of carboxylic acid ARIs.

Table 2. The lipophilicity of target compounds.

Cpd.	substituent		$\text{LogD}_{7.4}^a$	$\text{LogD}_{7.4} \text{ calc}^b$	$\text{pKa}_{7.4} \text{ calc}^b$
	R ¹	R ²			
6a	-COOH	H	0.82	1.78	6.10
6j	-COOH	3,5-(OH) ₂	0.57	0.74	5.94
7a	-CONHOH	H	1.53	2.27	8.93
7j	-CONHOH	3,5-(OH) ₂	1.32	1.66	8.73
8a	-CONHOCH ₃	H	1.19	2.00	6.51
8b	-CONHOCH ₃	3,5-(OH) ₂	0.73	1.38	6.57

9a	-CONHSO ₂ CH ₃	H	0.53	0.83	3.88
9b	-CONHSO ₂ CH ₃	3,5-(OH) ₂	*	0.22	5.63
epalrestat				-1.17	3.40

^a Distribution coefficient between n-octanol and aqueous buffer (pH=7.4) determined by LC/MS;

^b Calculated value by Chemaxon.

Compound **6j** endowed with excellent activities both on the AKR1B1 inhibition and antioxidant activity was docked with the conformation of the human AKR1B1/NADPH/zenarestat complex (PDB code:1IEI), and docking study of **7j** was also carried out to investigate whether the bioisostere strategy is feasible at molecular level.

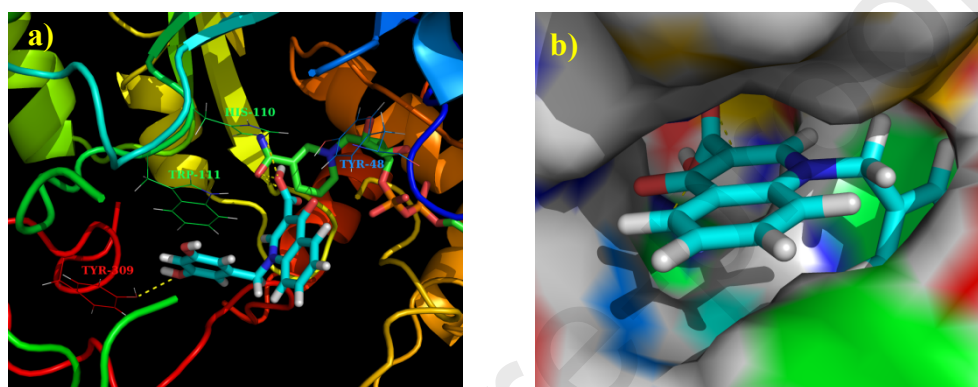


Figure 3 5. Docking of **6j** into the active site of AKR1B1. **(a)** The protein structure is shown in ribbon and tube representation with selected residues labeled and shown in line representation, ligand and NADP are shown as stick models. The docked pose of **6j** is shown in cyan (C), red (O) and blue (N). Hydrogen bonds are shown as yellow dashed lines. **(b)** Protein residues are in surface representation.

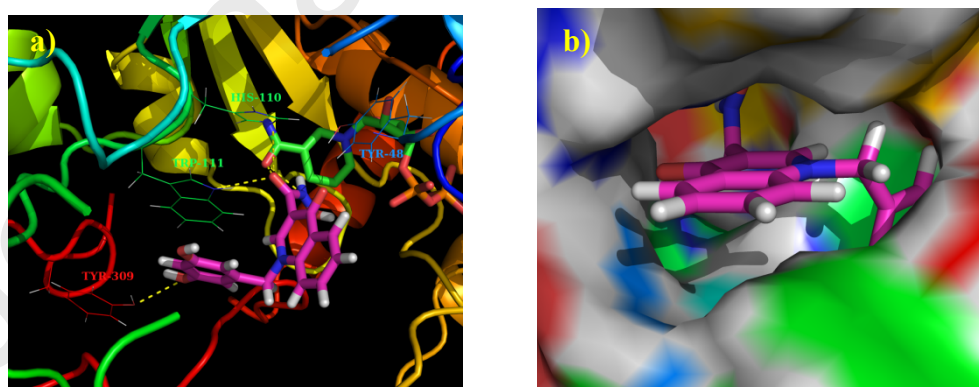


Figure 4 6. Docking of **7j** into the active site of AKR1B1. **(a)** The protein structure is shown in ribbon and tube representation with selected residues labeled and shown in line representation, ligand and NADP are shown as stick models. The docked pose of **7j** is shown in purple (C), red (O) and blue (N). Hydrogen bonds are shown as yellow dashed lines. **(b)** Protein residues are in surface representation.

As shown in **Fig. 3 5**, compound **6j** fitted suitably to the active site of AKR1B1.

The carboxylate group was inserted deeply in the anion binding site by forming tight hydrogen-bonding interaction with His110 (2.83 Å). Besides, the 3-hydroxyl oxygen atom at N1 aryl side chain formed an additional hydrogen bond with the side chain of Tyr309 (2.87 Å), confirming the importance of phenolic hydroxyl on the activity enhancement of AKR1B1 inhibition. Moreover, the 3,5-dihydroxy benzyl ring at N1 position was well placed into the specificity pocket and paralleled to the indole ring of Trp111 forming a stable stacking interaction. All those information at molecular level supported **6j** was endowed with a significant AKR1B1 inhibitory activity. The docking study of compound **7j** was described in Fig. 4 6, and the results indicated that a strong interaction between **7j** and AKR1B1 was also detected. The bioisostere hydroxamic acid group was inserted in the anion binding site and tight hydrogen-bonding interactions with the side chain of His110 (2.68 Å) and Trp111 (3.08 Å) were formed. Furthermore, the 3-hydroxyl oxygen atom at N1 aryl side chain formed an additional hydrogen bond with Tyr309 (2.94 Å), and the N1-benzyl ring was paralleled to the indole ring of Trp111. On this basis, it is reasonable to conclude that the hydroxamic acid group is feasible to be used as bioisostere of carboxylic acid in ARIs design.

In conclusion, a series of ARI candidates based on quinolin-4(1*H*)-one core structure were synthesized and biologically evaluated for AKR1B1 inhibition and selectivity, as well as anti-oxidative properties through DPPH radical scavenging test. To optimize the physicochemical profile of acetic acid ARIs, hydroxamic acid or acyl-sulfonamide moiety was used as bioisostere of acetic acid. The biological results showed that all compounds exhibited excellent AKR1B1 inhibitory activity in the IC₅₀ range of 0.057 to 15.034 μM. Compounds **6j** and **7j** containing phenolic 3,5-dihydroxyl on the N1 benzyl side chain were not only sufficient to inhibit AKR1B1 but also effective for DPPH radical scavenging, which indicated success in the development of potent ARIs with antioxidant activity. Excitedly, the hydroxamic acid derivative **7j** was also endowed with excellent lipophilicity and pKa value at physiological pH, which suggested that the bioisostere replacement of carboxylic acid ARI was successful. Further SAR and molecular docking studies highlighted the importance of hydroxamic acid head group along with phenolic hydroxyl substituent in N1 side chain of the scaffold for construction of potent and multi-effective ARIs with good physicochemical profile.

Acknowledgements

This work was supported by Funding for school-level research projects of Yancheng Institute of Technology (grant no. xjr2019013). The authors have no other relevant affiliations or financial involvement with any organization or entity with a financial interest in or financial

conflict with the subject matter or materials discussed in the manuscript apart from those disclosed.

References

- (1) Association, A. D.: Diagnosis and Classification of Diabetes Mellitus. **2012**, *101*, 274.
- (2) Sarwar, N.; Gao, P.; Seshasai, S. R.; Gobin, R.; Kaptoge, S.; Di, A. E.; Ingelsson, E.; Lawlor, D. A.; Selvin, E.; Stampfer, M.: Diabetes mellitus, fasting blood glucose concentration, and risk of vascular disease: a collaborative meta-analysis of 102 prospective studies. *The Lancet*, **2010**, *375*, 2215.
- (3) Whiting, D. R.; Leonor, G.; Clara, W.; Jonathan, S.: IDF Diabetes Atlas: Global estimates of the prevalence of diabetes for 2011 and 2030. **2011**, *094*, 0-321.
- (4) La Motta, C.; Sartini, S.; Salemo, S.; Simorini, F.; Taliani, S.; Marini, A. M.; Da Settimo, F.; Marinelli, L.; Limongelli, V.; Novellino, E.: Acetic acid aldose reductase inhibitors bearing a five-membered heterocyclic core with potent topical activity in a visual impairment rat model. *Journal of Medicinal Chemistry*, **2008**, *51*, 3182-3193.
- (5) Maccari, R.; Ottana, R.; Ciurleo, R.; Vigorita, M. G.; Rakowitz, D.; Steindl, T.; Langer, T.: Evaluation of in vitro aldose reductase inhibitory activity of 5-arylidene-2,4-thiazolidinediones. *Bioorganic & Medicinal Chemistry Letters*, **2007**, *17*, 3886-3893.
- (6) Stefek, M.; Soltsova Prnova, M.; Majekova, M.; Rechlin, C.; Heine, A.; Klebe, G.: Identification of Novel Aldose Reductase Inhibitors Based on Carboxymethylated Mercaptotriazinoindole Scaffold. *Journal of Medicinal Chemistry*, **2015**, *58*, 2649-2657.
- (7) Brownlee, M.: Biochemistry and molecular biology of diabetic complications. *Nature*, **2001**, *414*.
- (8) Hao, X.; Han, Z.; Li, Y.; Li, C.; Wang, X.; Zhang, X.; Yang, Q.; Ma, B.; Zhu, C.: Synthesis and structure-activity relationship studies of phenolic hydroxyl derivatives based on quinoxalinone as aldose reductase inhibitors with antioxidant activity. *Bioorganic & Medicinal Chemistry Letters*, **2017**, *27*, 887-892.
- (9) Chen, X.; Zhu, C.; Guo, F.; Qiu, X.; Yang, Y.; Zhang, S.; He, M.; Parveen, S.; Jing, C.; Li, Y.; Ma, B.: Acetic Acid Derivatives of 3,4-Dihydro-2H-1,2,4-benzothiadiazine 1,1-Dioxide as a Novel Class of Potent Aldose Reductase Inhibitors. *Journal of Medicinal Chemistry*, **2010**, *53*, 8330-8344.
- (10) Shukla, K.; Sonowal, H.; Saxena, A.; Ramana, K. V.; Srivastava, S. K.: Aldose reductase inhibitor, fidarestat regulates mitochondrial biogenesis via Nrf2/HO1/AMPK pathway in colon cancer cells. *Cancer Letters*, **2017**, *1*, 1-7.
- (11) Tammali, R.; Saxena, A.; Srivastava, S. K.; Ramana, K. V.: Aldose Reductase Inhibition Prevents Hypoxia-induced Increase in Hypoxia-inducible Factor-1 α (HIF-1 α) and Vascular Endothelial Growth Factor (VEGF) by Regulating 26 S Proteasome-mediated Protein Degradation in Human Colon Cancer Cells *. *Journal of Biological Chemistry*, **2011**, *27(286)*, 24089-24100.
- (12) Papastavrou, N.; Chatzopoulou, M.; Ballekova, J.; Cappiello, M.; Moschini, R.; Balestri, F.; Patsilidakos, A.; Ragno, R.; Stefek, M.; Nicolaou, I.: Enhancing activity and selectivity in a series of pyrrol-1-yl-1-hydroxypyrazole-based aldose reductase inhibitors: The case of trifluoroacetylation. *European Journal of Medicinal Chemistry*, **2017**, *130*, 328-335.
- (13) Kotsampasakou, E.; Demopoulos, V. J.: Synthesis of derivatives of the keto-pyrrolyl-difluorophenol scaffold: Some structural aspects for aldose reductase inhibitory activity and selectivity. *Bioorganic & Medicinal Chemistry*, **2013**, *21*, 869-873.

- (14) Ogawva, K.; Yamawaki, I.; Matsusita, Y. I.; Nomura, N.; Kador, P. F.; Kinoshita, J. H.: Syntheses of substituted 2,4-dioxo-thienopyrimidin-1-acetic acids and their evaluation as aldose reductase inhibitors. *European Journal of Medicinal Chemistry*, **1993**, *28*, 769-781.
- (15) Nencetti, S.; La Motta, C.; Rossello, A.; Sartini, S.; Nuti, E.; Ciccone, L.; Orlandini, E.: N-(Aroyl)-N-(arylmethoxy)- α -alanines: Selective inhibitors of aldose reductase. *Bioorganic & Medicinal Chemistry*, **2017**, *25*(12), 3068-3076.
- (16) Metwally, K.; Pratsinis, H.; Kletsas, D.; Quattrini, L.; Coviello, V.; Motta, C. L.; El-Rashedy, A. A.; Soliman, M. E. S.: Novel quinazolinone-based 2,4-thiazolidinedione-3-acetic acid derivatives as potent aldose reductase inhibitors. *Future Medicinal Chemistry*, **2017**, *9*(18), 2147-2166.
- (17) Chatzopoulou, M.; Patsilnakos, A.; Vallianatou, T.; Prnova, M.; Zakelj, S.; Ragno, R.; Stefek, M.; Kristl, A.; Kakoulidou, A.; Demopoulos, V.: Decreasing acidity in a series of aldose reductase inhibitors: 2-Fluoro-4-(1H-pyrrol-1-yl)phenol as a scaffold for improved membrane permeation. **2014**, *22*, 2194-2207.
- (18) Rakowitz, D.; Maccari, R.; Ottana, R.; Vigorita, M. G.: In vitro aldose reductase inhibitory activity of 5-benzyl-2,4-thiazolidinediones. *Bioorganic & Medicinal Chemistry* **2006**, *14*, 567-574.
- (19) Hao, X.; Qi, G.; Ma, H.; Zhu, C.; Han, Z.: Novel 2-phenoxyprido[3,2-b]pyrazin-3(4H)-one derivatives as potent and selective aldose reductase inhibitors with antioxidant activity. *Journal of Enzyme Inhibition and Medicinal Chemistry*, **2019**, *34*(1), 1368-1372.
- (20) Han, Z.; Hao, X.; Ma, B.; Zhu, C.: A series of pyrido[2,3-b]pyrazin-3(4H)-one derivatives as aldose reductase inhibitors with antioxidant activity. *European Journal of Medicinal Chemistry*, **2016**, *121*(2016), 308-317.
- (21) Zou, Y.; Qin, X.; Hao, X.; Zhang, W.; Han, Z.; Ma, B.; Zhu, Z.: Phenolic 4-hydroxy and 3,5-dihydroxy derivatives of 3-phenoxyquinoxalin-2(1H)-one as potent aldose reductase inhibitors with antioxidant activity. *Bioorganic & Medicinal Chemistry Letters*, **2015**, *25*(18), 3924-3927.
- (22) Qin, X.; Hao, X.; Han, H.; Zhu, S.; Yang, Y.; Wu, B.; Hussain, S.; Parveen, S.; Jing, C.; Ma, B. Zhu, C.: Design and Synthesis of Potent and Multifunctional Aldose Reductase Inhibitors Based on Quinoxalinones. *Journal of Medicinal Chemistry*, **2015**, *58*, 1254-1267.
- (23) Hussain, S.; Parveen, S.; Hao, X.; Zhang, S.; Wang, W.; Qin, X.; Yang, Y.; Chen, X.; Zhu, S.; Zhu, C.: Structure-activity relationships studies of quinoxalinone derivatives as aldose reductase inhibitors. *European Journal of Medicinal Chemistry*, **2014**, *80*, 383-392.

Declaration of interests

The authors declare that they have no known competing financial interests or personal relationships that could have appeared to influence the work reported in this paper.

The authors declare the following financial interests/personal relationships which may be considered as potential competing interests:

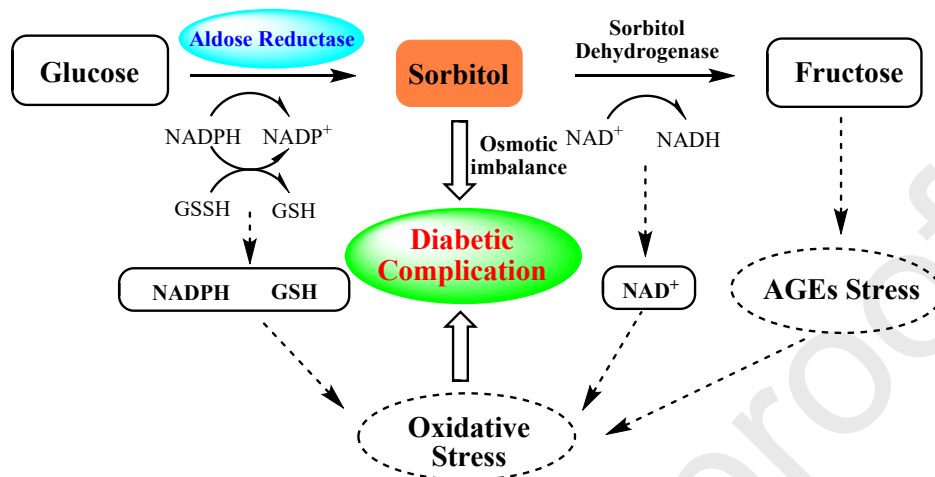


Figure 1. Polyol pathway of glucose metabolism.

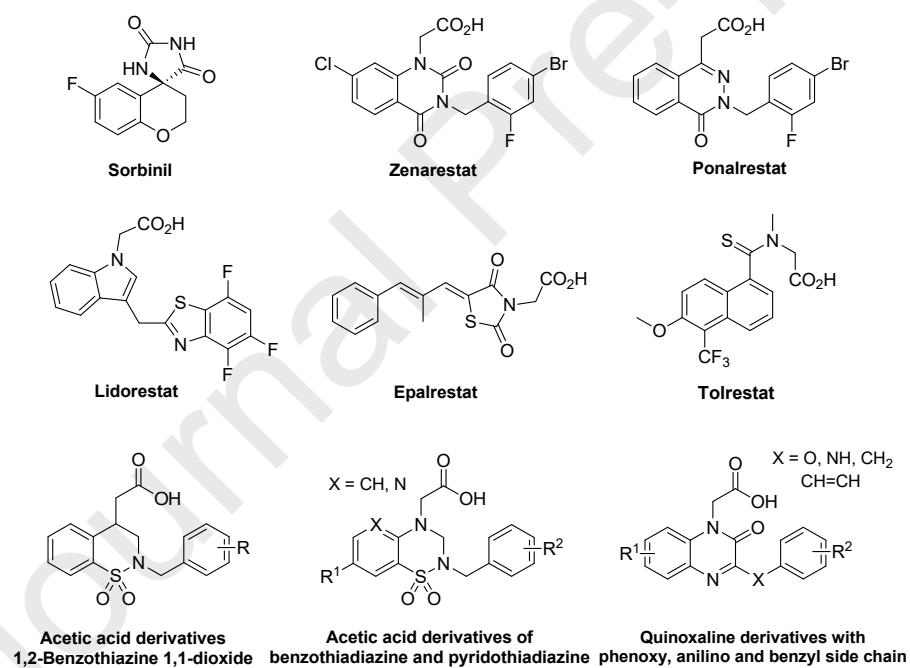


Figure 2. Structures of some ARIs.

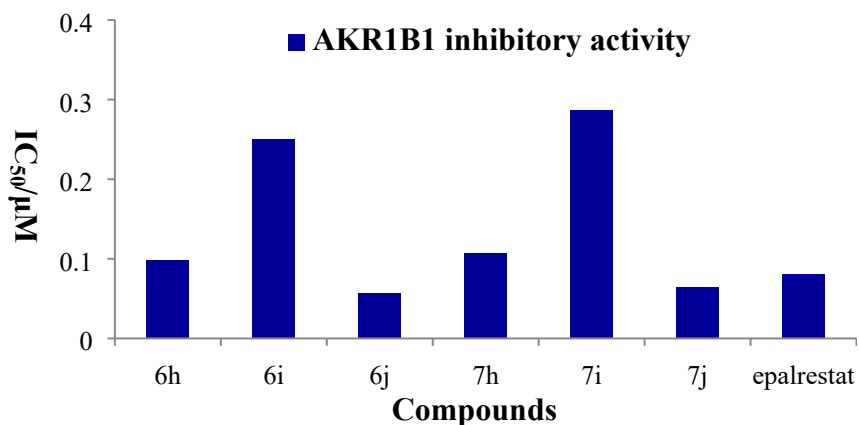


Figure 3. AKR1B1 inhibitory activity of some ARIs.

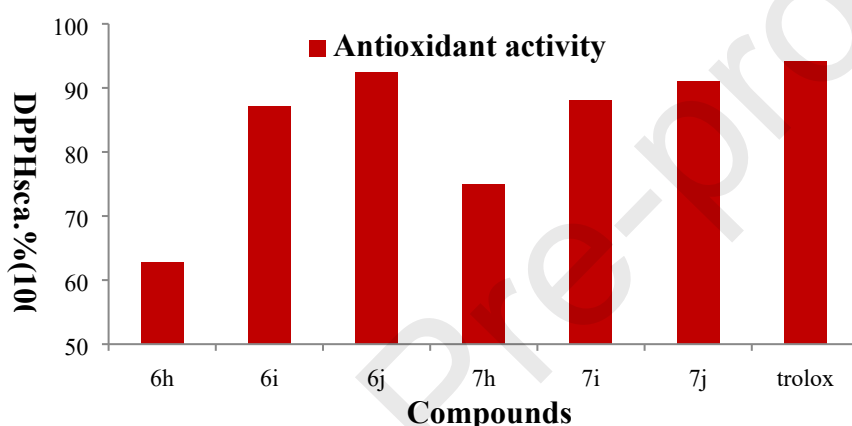


Figure 4. Antioxidant activity of some ARIs.

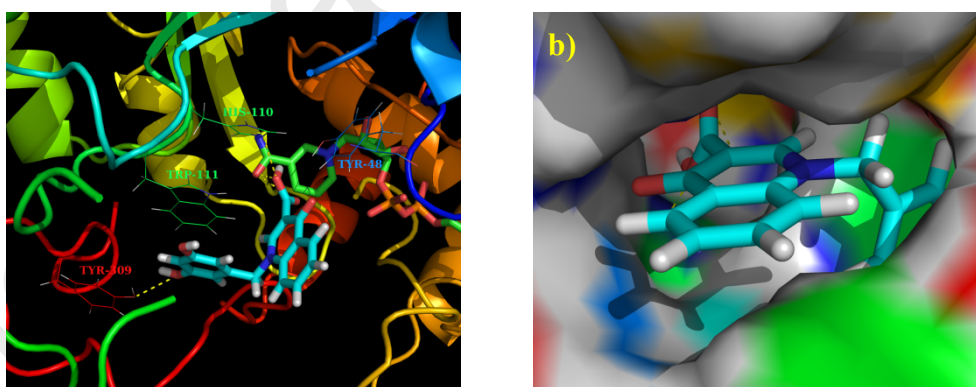


Figure 5. Docking of **6j** into the active site of AKR1B1. (a) The protein structure is shown in ribbon and tube representation with selected residues labeled and shown in line representation, ligand and NADP are shown as stick models. The docked pose of **6j** is shown in cyan (C), red (O) and blue (N). Hydrogen bonds are shown as yellow dashed lines. (b) Protein residues are in surface representation.

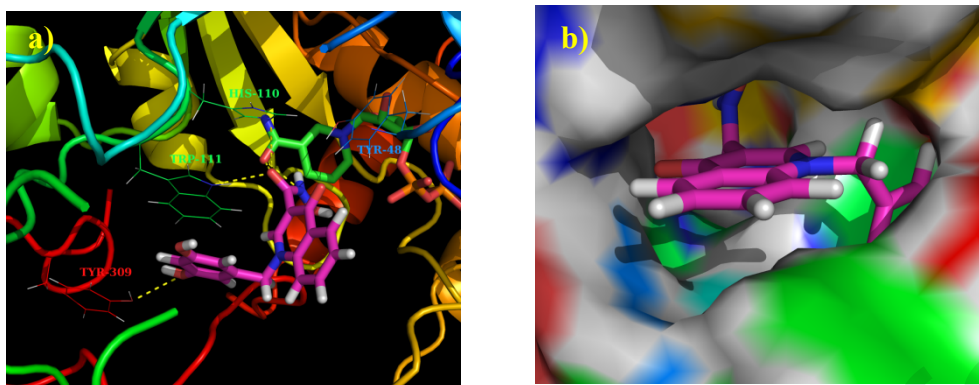
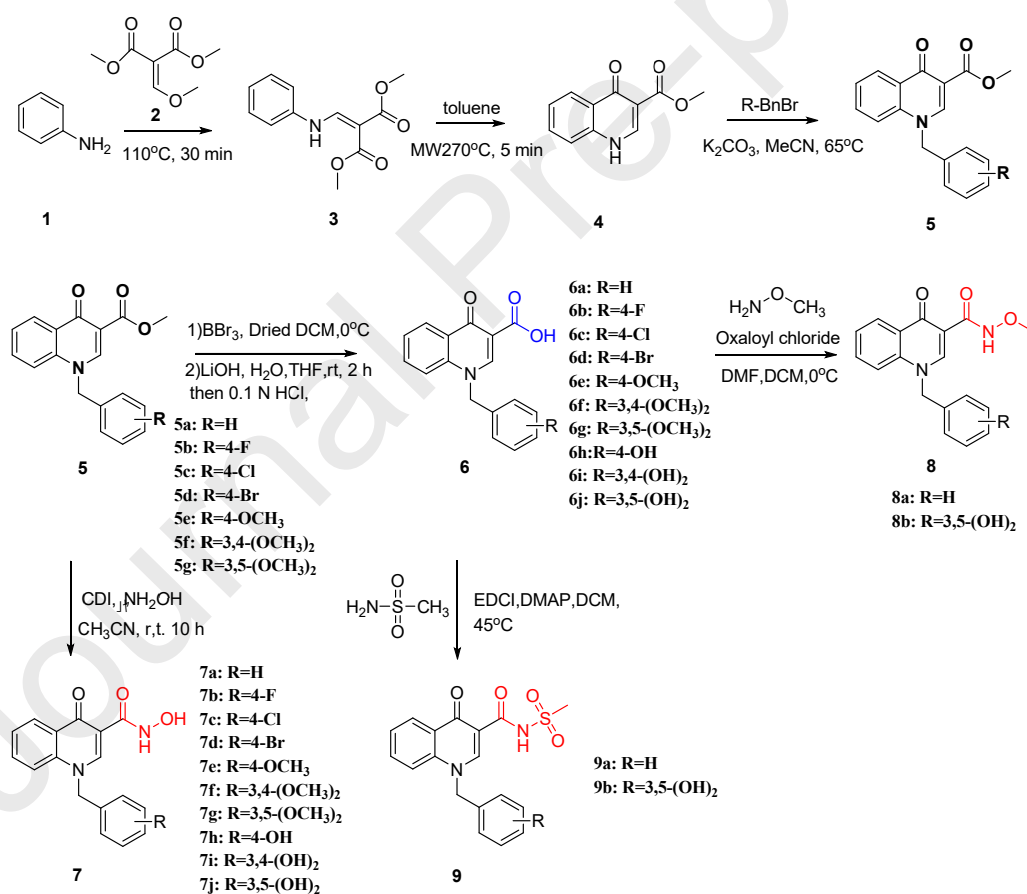
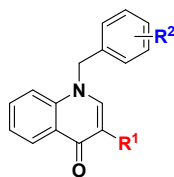


Figure 6. Docking of **7j** into the active site of AKR1B1. **(a)** The protein structure is shown in ribbon and tube representation with selected residues labeled and shown in line representation, ligand and NADP are shown as stick models. The docked pose of **7j** is shown in purple (C), red (O) and blue (N). Hydrogen bonds are shown as yellow dashed lines. **(b)** Protein residues are in surface representation.



Scheme 1. The synthetic route of target compounds.

Table 1. Biological activity of target compounds.



Cpd.	substituent		IC ₅₀ (μ M) ^a	Inhib(%) ^b		DPPH sca. %		
	R ¹	R ²		AKR1B1	AKR1A1	100 μ M	50 μ M	10 μ M
6a	-COOH	H	11.017 \pm 1.077	5.8	20.3 \pm 0.7	*	*	
6b	-COOH	4-F	0.154 \pm 0.012	30.2	21.4 \pm 0.9	*	*	
6c	-COOH	4-Cl	0.321 \pm 0.028	18.3	28.7 \pm 1.1	*	*	
6d	-COOH	4-Br	1.528 \pm 0.107	20.1	25.4 \pm 0.9	*	*	
6e	-COOH	4-OCH ₃	12.031 \pm 1.023	21.4	30.5 \pm 1.2	*	*	
6f	-COOH	3,4-(OCH ₃) ₂	10.587 \pm 1.005	24.8	32.2 \pm 1.3	*	*	
6g	-COOH	3,5-(OCH ₃) ₂	9.875 \pm 0.928	30.1	47.6 \pm 2.0	*	*	
6h	-COOH	4-OH	0.098 \pm 0.012	37.5	62.7 \pm 2.7	30.4 \pm 0.7	14.6 \pm 0.2	
6i	-COOH	3,4-(OH) ₂	0.251 \pm 0.022	38.6	87.1 \pm 3.4	61.9 \pm 1.2	44.9 \pm 2.1	
6j	-COOH	3,5-(OH) ₂	0.057 \pm 0.005	36.6	92.4 \pm 3.3	71.1 \pm 1.5	51.7 \pm 2.5	
7a	-CONHOH	H	12.578 \pm 1.069	7.1	27.1 \pm 0.9	*	*	
7b	-CONHOH	4-F	0.237 \pm 0.023	24.1	32.1 \pm 1.1	*	*	
7c	-CONHOH	4-Cl	0.626 \pm 0.059	26.5	31.7 \pm 1.0	*	*	
7d	-CONHOH	4-Br	2.487 \pm 0.186	17.6	27.6 \pm 0.8	*	*	
7e	-CONHOH	4-OCH ₃	12.515 \pm 1.089	7.6	34.1 \pm 1.3	*	*	
7f	-CONHOH	3,4-(OCH ₃) ₂	13.578 \pm 1.039	10.5	39.1 \pm 1.4	*	*	
7g	-CONHOH	3,5-(OCH ₃) ₂	15.614 \pm 1.202	17.2	41.3 \pm 1.5	*	*	
7h	-CONHOH	4-OH	0.107 \pm 0.008	34.6	74.9 \pm 2.4	51.1 \pm 1.9	32.3 \pm 1.5	
7i	-CONHOH	3,4-(OH) ₂	0.287 \pm 0.215	25.4	88.1 \pm 3.1	65.1 \pm 2.4	51.1 \pm 2.0	
7j	-CONHOH	3,5-(OH) ₂	0.065 \pm 0.005	27.4	91.0 \pm 3.1	72.4 \pm 2.6	57.8 \pm 2.1	
8a	-CONHOCH ₃	H	12.781 \pm 1.163	5.1	25.2 \pm 0.8	*	*	
8b	-CONHOCH ₃	3,5-(OH) ₂	0.689 \pm 0.057	21.7	88.7 \pm 3.0	55.8 \pm 2.4	42.7 \pm 1.8	
9a	-CONHSO ₂ CH ₃	H	15.034 \pm 1.353	7.9	28.7 \pm 1.1	*	*	
9b	-CONHSO ₂ CH ₃	3,5-(OH) ₂	0.112 \pm 0.010	24.7	79.4 \pm 3.1	64.7 \pm 3.1	33.6 \pm 1.1	
epalrestat			0.081 \pm 0.007	43.1	*	*	*	
Trolox					94.2 \pm 1.9	84.1 \pm 1.2	77.2 \pm 0.2	
				*				

^a IC₅₀ values represent the concentration required to produce 50% enzyme inhibition.

^b The inhibitory effect was estimated at a concentration of 10 μ M.

* Not tested.

Table 2. The lipophilicity of target compounds.

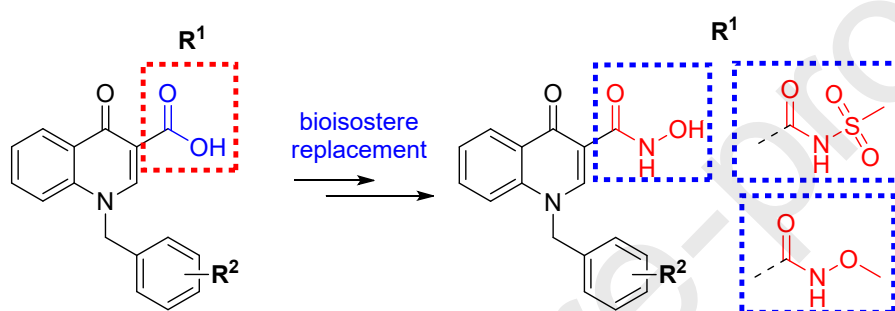
Cpd.	substituent		LogD _{7.4} ^a	LogD _{7.4} calc ^b	pKa _{7.4} calc ^b
	R ¹	R ²			
6a	-COOH	H	0.82	1.78	6.10
6j	-COOH	3,5-(OH) ₂	0.57	0.74	5.94
7a	-CONHOH	H	1.53	2.27	8.93

7j	-CONHOH	3,5-(OH) ₂	1.32	1.66	8.73
8a	-CONHOCH ₃	H	1.19	2.00	6.51
8b	-CONHOCH ₃	3,5-(OH) ₂	0.73	1.38	6.57
9a	-CONHSO ₂ CH ₃	H	0.53	0.83	3.88
9b	-CONHSO ₂ CH ₃	3,5-(OH) ₂	*	0.22	5.63
epalrestat				-1.17	3.40

^a Distribution coefficient between n-octanol and aqueous buffer (pH=7.4) determined by LC/MS;

^b Calculated value by Chemaxon.

Graphical Abstract



$R^2 = \text{H}, 4\text{-X}, 4\text{-OCH}_3, 4\text{-OH}, 3,4\text{-(OH)}_2, 3,5\text{-(OH)}_2$

IC₅₀ for AKR1B1: 0.057-15.614 μM

DPPH Radical Scavenging in 100 μM : 20.3-92.4%